

Molecular Transport | Hot Paper |



Naphthalene Imide Conjugates: Formation of Supramolecular Assemblies, and the Encapsulation and Release of Dyes through DNA-Mediated Disassembly

Balaraman H. Shankar,^[a] Dhanya T. Jayaram,^[a] and Danaboyina Ramaiah ^{*[a, b]}

Abstract: We report the synthesis of two new amphiphilic conjugates **1** and **2** based on naphthalene di- and mono-imide chromophores and the investigation of their photophysical, self-assembly and DNA-binding properties. These conjugates showed aqueous good solubility and exhibited strong interactions with DNA and polynucleotides such as poly(dG-dC)-poly(dG-dC) and poly(dA-dT)-poly(dA-dT). The interaction of these conjugates with DNA was evaluated by photo- and biophysical techniques. These studies revealed that the conjugates interact with DNA through intercalation with association constants in the order of $5\text{--}8 \times 10^4 \text{ M}^{-1}$. Of

these two conjugates, bolaamphiphile **1** exhibited a supramolecular assembly that formed vesicles with an approximate diameter of 220 nm in the aqueous medium at a critical aggregation concentration of 0.4 mM, which was confirmed by SEM and TEM. These vesicular structures showed a strong affinity for hydrophobic molecules such as Nile red through encapsulation. Uniquely, when exposed to DNA the vesicles disassembled, and therefore this transformation could be utilised for the encapsulation and release of hydrophobic molecules by employing DNA as a stimulus.

Introduction

The self-assembly of amphiphilic conjugates has been an active area of interest in recent years due to their medicinal and material applications.^[1] Thus, small-molecule based amphiphiles, such as surfactants, bolaamphiphiles and gemini surfactants, have been employed to generate diverse nanostructures (e.g., micelles, vesicles, fibres and nanotubes).^[2] Most of these amphiphiles contain hydrophobic and hydrophilic segments, which are known to form various supramolecular assemblies in organic media through various non-covalent interactions.^[3] However, creating well-defined nanostructures in aqueous media for efficient biological applications is a great challenge. In this context, supramolecular assemblies of appropriately substituted chemical building blocks (such as amphiphilic and bolaamphiphilic systems) have attracted much attention.^[4]

Recently, increasing efforts are being made towards the development of stimuli-responsive units that contain

well-defined nanostructures because of their advantages over conventional structures. In general, the stimulus employed to generate the desired nanoarchitecture can be a change in temperature, pH, light, magnetic field or ionic strength of the medium.^[5] Among the various stimuli investigated, materials that respond to biological stimuli, such as proteins and nucleic acids, have been less explored.^[6] Therefore, the design of functional chromophores that form supramolecular assemblies with biomolecule-responsive architectures in aqueous media is quite challenging. Of the various chromophores, systems based on naphthalene imides are very attractive biomolecule-responsive units because they have extended π systems and belong to an important class of DNA-binding agents.^[7]

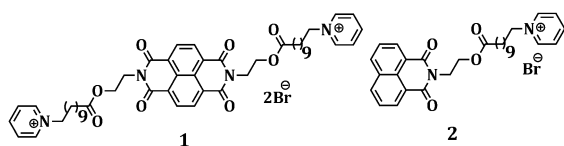
In this context, we have designed two amphiphilic conjugates **1** and **2** based on naphthalene imides and have investigated their photophysical, self-assembly and DNA-responsive properties. The uniqueness of these conjugates is their amphiphilic nature, thus they are expected to exhibit good aqueous solubility. The presence of the planar π -extended aromatic surface in these systems makes them interesting candidates to explore the formation of bioresponsive supramolecular assemblies in aqueous media. Our investigations have revealed that both conjugates **1** and **2** exhibited good solubility in the aqueous medium and had a strong affinity for DNA and polynucleotides through intercalation. Of these two conjugates, bolaamphiphile **1** formed vesicular structures above the critical aggregate concentration (CAC) of 0.4 mM, which could encapsulate hydrophobic dye molecules. Interestingly, these supramolecular vesicular structures of conjugate **1** disassembled in the presence of DNA, and this DNA-mediated transformation could

[a] B. H. Shankar, Dr. D. T. Jayaram, Dr. D. Ramaiah
Photosciences and Photonics Section
Chemical Sciences and Technology Division
CSIR-National Institute for Interdisciplinary Science and
Technology (CSIR-NIIST), Trivandrum 695 019 (India)
E-mail: rama@niist.res.in
d.ramaiah@gmail.com

[b] Dr. D. Ramaiah
CSIR-North East Institute of Science and Technology (CSIR-NEIST)
Jorhat 785 006, Assam (India)
E-mail: rama@rrl.jorhat.res.in

Supporting information for this article is available on the WWW under
<http://dx.doi.org/10.1002/chem.201502955>. It contains detailed synthetic
procedures and characterisation data for compounds **1** and **2**.

be effectively utilised to encapsulate and release dyes in the aqueous medium.



Results and Discussion

Synthesis

Symmetric bolaamphiphile **1** was synthesised from naphthalenetetracarboxylic dianhydride (**NDA**) in three steps (Scheme S1, see the Supporting Information). **NDA** reacted with ethanolamine to afford the corresponding alcohol derivative, which was successively esterified with 11-bromoundecanoic acid (2 equiv) and quaternised with pyridine to give bolaamphiphile **1** in moderate yield ($\approx 66\%$). Similarly, the synthesis of amphiphilic naphthalimide derivative **2** was achieved in moderate yield ($\approx 55\%$) (Scheme S2, see the Supporting Information) starting from naphthalic anhydride (**NMA**). Amination of **NMA** with ethanolamine, followed by esterification and subsequent quaternisation with pyridine yielded conjugate **2**. All these starting materials and products were purified and unambiguously characterised by various analytical and spectroscopic techniques.

Photophysical and self-assembly properties

We investigated the photophysical properties, including time-resolved fluorescence spectral analysis, of both conjugates under different conditions. For example, the ground-state absorption spectrum of conjugate **1** in the aqueous medium showed characteristic vibrationally resolved spectral bands of the naphthalene diimide (NDI) chromophore ($\lambda_{\text{max}} = 382 \text{ nm}$, $\epsilon = 2.33 \pm 0.1 \times 10^4 \text{ M}^{-1} \text{ cm}^{-1}$; Figure 1). For conjugate **2** we observed the absorption maximum at $\lambda = 344 \text{ nm}$ ($\epsilon = 1.42 \pm 0.1 \times 10^4 \text{ M}^{-1} \text{ cm}^{-1}$). In the fluorescence spectra **1** and **2** showed maxima at $\lambda = 390$ and 378 nm , respectively. The fluorescence quantum yields (Φ_{F}) of these conjugates were determined in the aqueous medium. We observed significantly quenched

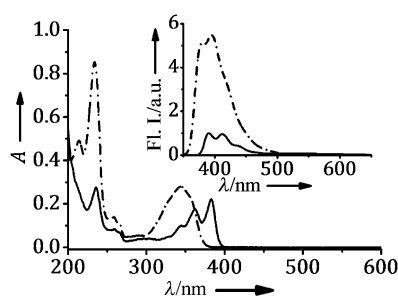


Figure 1. Absorption and emission (inset) spectra of conjugates **1** ($10 \mu\text{M}$; —) and **2** ($20 \mu\text{M}$; ----) in the aqueous medium. $\lambda_{\text{ex}} = 360$ and 345 nm , respectively.

values for diimide conjugate **1** ($\Phi_{\text{F}} = 0.005$), relative to monoimide derivative **2** ($\Phi_{\text{F}} = 0.29$), which indicated an efficient intensity quenching for **1**, as reported in the literature.^[8]

To determine the excited-state behaviour of conjugates **1** and **2** we carried out picosecond time-resolved fluorescence measurements. The fluorescence lifetime (τ), in the case of conjugate **1**, was found to be very short lived ($\tau < 0.1 \text{ ns}$), which is a characteristic feature of the N-substituted NDI chromophore.^[9] The fluorescence decay profile of conjugate **2** ($\lambda_{\text{ex}} = 335 \text{ nm}$) resulted in a mono-exponential decay profile with an emission lifetime of about $2.2 \pm 0.3 \text{ ns}$. This value can be attributed to the local excited state (monomer) emission of the naphthalimide chromophore^[10] (Figure S1, see the Supporting Information).

To understand the propensity of the conjugates under investigation to aggregate we monitored the absorption and fluorescence properties of **1** and **2** at higher concentrations. Figure 2 shows the concentration-dependent absorption and

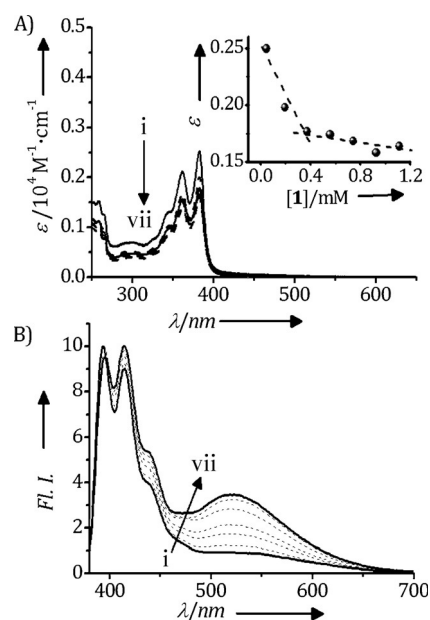


Figure 2. Concentration-dependent A) absorption and B) emission spectra (normalised) of conjugate **1** in the aqueous medium. $c = \text{i) } 46 \mu\text{M}$ to $\text{vii) } 1.1 \text{ mM}$. Inset: shows the variation of the extinction coefficient at $\lambda = 380 \text{ nm}$ as a function of the concentration of conjugate **1**. Path length of the cell (l) = 0.1 cm , $\lambda_{\text{ex}} = 360 \text{ nm}$.

emission spectra of conjugate **1**. As the concentration was increased from $46 \mu\text{M}$ to 1.1 mM , we observed a deviation from linearity at concentrations greater than about 0.4 mM . The CAC of **1** was estimated from the change in the concentration-dependent molar extinction coefficient (ϵ) at $\lambda = 382 \text{ nm}$ to be 0.4 mM (Figure 2A, inset). In the emission spectrum, we observed a gradual increase in the emission at $\lambda = 510 \text{ nm}$ as the concentration increased, with the I_{510}/I_{390} ratio varying from 0.2 to 0.9. Similar observations were made for conjugate **2** (CAC $\approx 0.25 \text{ mM}$). In the emission studies, we observed the formation of a new band at $\lambda = 500 \text{ nm}$. When monitored at $\lambda = 510 \text{ nm}$, conjugate **1** (at the CAC) decayed bi-exponentially

with an average fluorescence lifetime ($\langle\tau\rangle$) of 3.3 ± 0.2 ns, which can be attributed to formation of the intermolecular excimer of the NDI (Figure S2, see the Supporting Information). Similarly, conjugate **2** (at the CAC) showed a bi-exponential decay with $\tau = 22.6 \pm 0.1$ (90%) and 4.11 ± 0.2 ns (10%), which can be attributed to the excimer and monomer of the naphthalimide unit, respectively.

To understand the observation of excimer emission at higher concentrations and the supramolecular assemblies formed, we carried out morphological analysis of conjugates **1** and **2** through dynamic light scattering (DLS), SEM and TEM techniques. At lower concentrations (< 0.4 mM, i.e. below the CAC), bolaamphiphile **1** showed negligible formation of nano-aggregates (assessed by particle size analysis). Interestingly, at the CAC (0.4 mM) we observed aggregates with a Z-average hydrodynamic diameter of 240 nm with good correlation data (Figure S3, see the Supporting Information). In contrast, amphiphilic conjugate **2** at CAC did not show good correlation data, which indicates that the aggregates formed from this system were not spherical. To evidence these observations, we carried out SEM and TEM analysis and the images from both these techniques confirmed the formation of self-assembled structures of **1** with diameters of approximately 220 ± 5 nm.

To get more insight into the nature of the self-assembled structure of conjugate **1**, we carried out TEM analysis after negative staining with phosphotungstic acid (pH 7.4). The images obtained revealed the presence of spherical particles with distinctive walls approximately 5 nm wide and a solid interior, which confirmed that the self-assembled structures formed were vesicular in nature (Figure 3A and b). The thickness of the walls closely matched the theoretically calculated extended-aliphatic-chain length of conjugate **1** (Figure S4a, see the Supporting Information). The formation of vesicles can be rationalised as a result of the cumulative effect of π -stacking interactions between the NDI chromophore and the curvature provided by minimising exposure of the central hydro-

phobic chain to water (Figure S4b, see the Supporting Information).^[11a] In contrast, SEM and TEM analysis showed that amphiphilic derivative **2** formed lamellar flakes (Figure S5, see the Supporting Information), due to the absence of the curved structure required to form vesicular aggregates. These results agreed with the data obtained by particle analysis.

To evaluate the potential utility of the vesicles as drug-carrier systems, we studied their interactions with a hydrophobic dye, Nile red, which has negligible solubility in the aqueous medium. The emission spectrum of Nile red ($c = 100 \mu\text{M}$) was monitored for a series of solutions with varying concentrations of conjugate **1**. We observed a strong emission at $\lambda = 630$ nm, which corresponded to Nile red encapsulated in the vesicles of **1** (Figure 3C). Furthermore, the emission intensity of Nile red at $\lambda = 630$ nm was monitored as a function of the concentration of **1**. From the inflection point of the plot, we obtained a CAC of 0.4 mM, which is in agreement with that obtained for **1** from the absorption studies. The encapsulation of Nile in the hydrophobic micro-environment of the vesicles of the **1** is confirmed by a bi-exponential emission decay profile with $\tau = 10.05 \pm 0.2$ and 2.1 ± 0.1 ns (cf. Nile red in THF: $\tau = 4.1 \pm 0.4$ ns). The long-lived encapsulated Nile red species can be attributed to storage of dye molecules inside the hydrophobic part of the vesicles, whereas the short-lived species could be due to molecules located at the interphase between the aqueous medium and the vesicles.^[11b] Further evidence for the encapsulation was obtained by observation of red-light-emitting spherical particles in a solution of vesicle-encapsulated Nile red in the aqueous medium that was examined under a fluorescence microscope (Figure 3D).

DNA-binding properties

To investigate the potential of biomolecules as stimuli, we studied the interactions of the conjugates with proteins [for example, bovine serum albumin (BSA)], calf thymus (ct) DNA and synthetic polynucleotides at different concentrations. The successive addition of BSA (0–50 μM) led to negligible changes in the absorption and fluorescence spectra of conjugate **1** (10 μM) in buffer (Figure S6, see the Supporting Information). Similar observations were made for conjugate **2**. These observations indicate that the conjugates undergo less-efficient interactions with albumins. In contrast, the addition of ct-DNA (0–50 μM) in small aliquots to a solution of conjugate **1** (10 μM) in buffer resulted in a gradual decrease of the absorbance at $\lambda = 382$ nm, which corresponds to the NDI chromophore (Figure 4A). Maximum hypochromicity ($\approx 42\%$) was observed at a DNA concentration of 50 μM , along with a bathochromic shift of about 3 nm with isosbestic points at $\lambda = 389$ and 313 nm. The intrinsic binding constant (K_{DNA}) was calculated by half-reciprocal analysis ($K_{\text{DNA}} = 8.61 \pm 0.03 \times 10^4 \text{ M}^{-1}$), which indicates the strong binding affinity of conjugate **1** towards DNA.

As the concentration of DNA increased we observed a regular and significant decrement of the fluorescence intensity at $\lambda = 390$ nm (the NDI monomer) in the emission spectra of conjugate **1**. We observed a concomitant enhancement of the

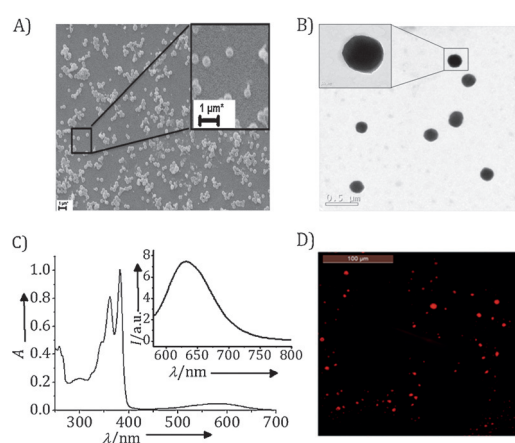


Figure 3. A) SEM and B) TEM images of vesicles of **1** in the aqueous medium ($c = 0.4$ mM). Insets: magnified images of the portion marked by the black box in the respective images. C) Absorption and emission (inset) spectra of an aqueous solution of **1** (0.4 mM) containing Nile red (100 μM). D) Fluorescence microscopic images of Nile red encapsulated in vesicles of conjugate **1** in the aqueous medium. $\lambda_{\text{ex}} = 530$ nm.

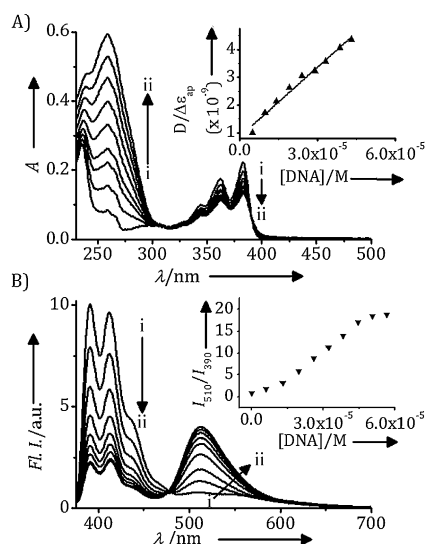


Figure 4. Changes in the A) absorption and B) emission spectra of **1** (10 μM) in the presence of ct-DNA in phosphate buffer (10 mM, pH 7.4) containing NaCl (2 mM). [DNA] = i) 0 and ii) 50 μM . Insets: a) half-reciprocal analysis for the binding of **1** with DNA and b) ratiometric plot between these emission maxima at $\lambda = 510$ and 390 nm. $\lambda_{\text{ex}} = 362$ nm.

emission intensity at $\lambda = 510$ nm, which is attributed to excimer formation (Figure 4B). At a 50 μM DNA concentration, we observed about 30-fold enhancement of the I_{510}/I_{390} ratio, which led to DNA recognition in the buffer medium through the excimer emission of conjugate **1**. Similarly, we observed a significant hypochromicity ($\approx 39\%$) in the absorption spectra of conjugate **2** (20 μM) upon addition of DNA (73 μM). In the emission spectra of **2**, we observed a prominent and gradual decrease in the peak intensity at $\lambda = 378$ nm, with a concomitant peak enhancement at $\lambda = 500$ nm (Figure S7 a, see the Supporting Information). The K_{DNA} value between conjugate **2** and DNA was $5.56 \pm 0.1 \times 10^4 \text{ M}^{-1}$, determined by half-reciprocal analysis.^[12] The K_{DNA} value of bolaamphiphilic conjugate **1** was about 1.6-fold higher than that of conjugate **2**. This is due to the presence of two cationic charges in the former versus a single cationic charge in the latter.

To evaluate the effect of DNA on the excited-state properties, we analysed the fluorescence decay profiles of conjugates **1** and **2** under different conditions. The successive addition of DNA aliquots to a solution of conjugate **1** in buffer resulted in a gradual increase in the fluorescence lifetime when monitored at $\lambda = 510$ nm. A significant enhancement to $\tau = 2.49$ ns (initial $\langle \tau \rangle = 0.1$ ns) was observed in the presence of DNA (50 μM) (Figure S7 b, see the Supporting Information). In contrast, we observed negligible changes of the fluorescence lifetimes of conjugate **2**, which corresponded to monomeric emission at $\lambda = 378$ nm, even at a 73 μM DNA concentration. However, when we monitored the emission at $\lambda = 500$ nm we observed a bi-exponential fluorescence decay profile with $\tau = 2.5 \pm 0.02$ (31 %) and 17.2 ± 0.07 ns (69%), which correspond to the monomer and excimer of the naphthalimide chromophore, respectively.

To understand the origin of the excimer emission, we employed time-resolved emission spectroscopy (TRES). TRES analysis of conjugate **1** showed a single peak at $\lambda = 395$ nm (NDI monomer) immediately after excitation (7 ps). However, in the presence of DNA (50 μM) excimer formation was observed, even at 63 ps, and it showed an intensity enhancement as a function of time. After a 1 ns excitation pulse, the spectrum was dominated exclusively by the excimer emission ($\lambda_{\text{max}} = 510$ nm). Similar observations were made for conjugate **2** in the presence of DNA (Figure 5; Table S1, see the Supporting Information).

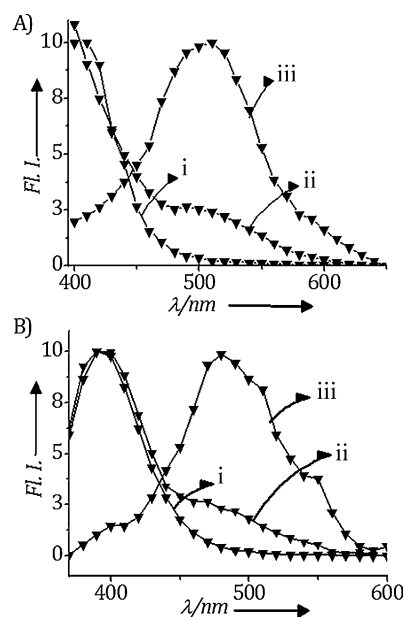


Figure 5. Time-resolved emission spectra (TRES) of conjugates A) **1** (10 μM) and B) **2** (20 μM) in the presence of DNA (50 μM) in phosphate buffer (10 mM, pH 7.4) monitored after an excitation pulse of i) 7 ps; 0.5 ns, ii) 63 ps; 1.4 ns, and iii) 1.4 ns; 13.8 ns. $\lambda_{\text{ex}} = 375$ and 335 nm, respectively.

To evaluate the DNA-sequence selectivity, we investigated the interactions of conjugates **1** and **2** with synthetic polyoligonucleotides poly(dG-dC)-poly(dG-dC) and poly(dA-dT)-poly(dA-dT). Addition of increasing aliquots of poly(dG-dC)-poly(dG-dC) to a solution of conjugate **1** in buffer showed an enhancement of the excimer emission at $\lambda = 510$ nm (Figure S8, see the Supporting Information) and a concomitant decrease of the monomer emission. As in the case of ct-DNA, we determined the association constant ($K_{\text{DNA}} = 3.52 \pm 0.2 \times 10^5 \text{ M}^{-1}$). Similar observations were made for conjugate **2** ($K_{\text{DNA}} = 1.71 \pm 0.1 \times 10^5 \text{ M}^{-1}$). The addition of poly(dA-dT)-poly(dA-dT) to **1** also led to similar ratiometric changes, albeit with lower affinity ($K_{\text{DNA}} = 1.4 \pm 0.2 \times 10^4 \text{ M}^{-1}$). These results indicate that conjugates **1** and **2** show strong sequence dependency, and the efficiency was in the order: poly(dG-dC)-poly(dG-dC) > ct-DNA > poly(dA-dT)-poly(dA-dT). This sequence dependency can be attributed to the relatively low ionisation potential of the GC pair relative to the AT sequences, as reported in the literature.^[13]

Nature of the DNA-binding interactions

To determine the nature of the interactions of the conjugates with DNA, we studied the effect of the ionic strength of the medium. With successive addition of aliquots of DNA to a solution of **1** in buffer containing NaCl (2 or 50 mM) we observed a lower I_{510}/I_{390} ratio at the higher NaCl concentration. When the DNA-binding studies were carried out in a buffer that contained NaCl (500 mM), we observed only negligible changes in the DNA-mediated excimer emission of conjugate **1**. The association constants for these interactions were calculated in solution in a buffer that contained NaCl (50, 100 or 500 mM) as $K_{\text{DNA}} = 1.15, 0.85$ and $0.71 \times 10^4 \text{ M}^{-1}$, respectively. Similar observations were made for conjugate **2**: $K_{\text{DNA}} = 0.75, 0.58$ and $0.41 \times 10^4 \text{ M}^{-1}$ in the presence of NaCl (50, 100 or 500 mM), respectively. These observations clearly suggest that electrostatic interactions play an important role in the binding interactions of conjugates **1** and **2** with DNA.

The DNA-binding affinities of **1** and **2** were further investigated by employing the competitive ethidium bromide (EB) binding assay.^[14] For example, a 2.4-fold emission enhancement was observed at $\lambda = 630 \text{ nm}$ after addition of ct-DNA to EB, which corresponded to formation of an EB–DNA complex ($K_{\text{DNA}} = 1.23 \pm 0.07 \times 10^5 \text{ M}^{-1}$).^[14b] Subsequent addition of conjugate **1** to this EB–DNA complex, showed approximately a 1.7-fold ($\approx 70\%$) decrease in the emission intensity (Figure S9, see the Supporting Information). Similarly, amphiphilic conjugate **2** showed an approximately 1.5-fold ($\approx 62\%$) decrease in the emission intensity of the EB–DNA complex. These results corroborate that both **1** and **2** can efficiently displace EB, possibly due to their intercalative mode of interaction.

We employed circular dichroism (CD) spectroscopy, viscosity and thermal denaturation analysis to further understand the nature of the interactions. The CD spectrum of ct-DNA consists of distinctive peaks at $\lambda = 280$ (+ve) and 245 nm (–ve) (Figure S10a, see the Supporting Information). Upon addition of conjugate **1** to a solution of ct-DNA in buffer, a bisignated CD signal with maxima at $\lambda = 363$ (+ve) and 411 nm (–ve) was observed. Both these bands are located on either side of the absorption maximum of the free conjugate **1** ($\lambda = 382 \text{ nm}$). This observation could be attributed to exciton coupling between the planar NDI aromatic surfaces at the intercalative sites.^[15] Although the exciton CD signals are not characteristic features of intercalators (the nearest-neighbour exclusion principle), few classical intercalators that show distinctive bisignated bands are reported in the literature.^[15b] However, amphiphilic derivative **2** showed a negative ICD signal ($\lambda_{\text{max}} = 344 \text{ nm}$), which is typically observed for intercalators,^[16] with transition moments perpendicular to the DNA longitudinal axis (Figure S10b, see the Supporting Information).

Changes in the dynamic viscosity of DNA were monitored with increasing conjugate concentration. We observed a value of $1.1 \pm 0.02 \text{ mPa s}$ for ct-DNA (0.3 mM) in buffer at 25 °C, which gradually increased to 1.57 ± 0.01 and $1.43 \pm 0.01 \text{ mPa s}$ in the presence of conjugate **1** (0.1 mM) or **2** (0.1 mM), respectively, under identical conditions. The viscosity changes observed indicate that these systems undergo an intercalative

binding mode, similar to reported examples.^[17] Further, the melting temperature of synthetic polynucleotide poly(dA-dT)–poly(dA-dT) ($T_m = 44$ °C) substantially increased to 66 or 54 °C in the presence of conjugates **1** and **2**, respectively (Figure 6), which indicated that both **1** and **2** significantly stabilise the duplex, predominantly through intercalative interactions.^[18]

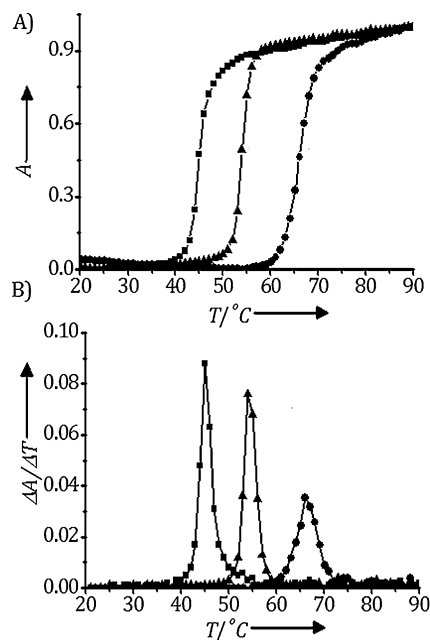


Figure 6. A) Thermal denaturation and B) differential thermal denaturation curves for poly(dA-dT)–poly(dA-dT) (8.3 μM), in the absence (\blacksquare ; $T_m = 44$ °C) and presence of conjugate **1** (\bullet ; 8.3 μM , $T_m = 66$ °C) and **2** (\blacktriangle ; 8.3 μM , $T_m = 54$ °C). Absorbance monitored at $\lambda = 260 \text{ nm}$.

DNA-mediated disassembly of the vesicles

To evaluate the potential of DNA as a stimulus, we investigated the interactions of DNA with vesicles of conjugate **1** formed at the CAC (0.4 mM). Interestingly, upon addition of DNA (0.3 mM) to vesicles of **1** in solution in buffer we observed significant hypochromicity ($\approx 36\%$) in the absorption spectrum. In the emission spectrum, we observed significant enhancement of the excimer intensity ($I_{510}/I_{390} = 1.6$; Figure S11, see the Supporting Information), which indicated disruption of the vesicles under these conditions. To obtain evidence for this transformation, we carried out morphological analysis of the vesicles in the presence of DNA through DLS and TEM techniques (without negative staining). As shown in Figure 7A, we observed prominent changes in the size-distribution curves and the amplitude of the correlogram in the presence of DNA (0.4 mM) (Figure 7A and b; ii). Under these conditions, TEM images indicated only reticulated fibres that were about 300 nm wide (Figure 7C), which confirmed vesicle disassembly. Furthermore, we utilised the disruption of the vesicles to release the encapsulated dye molecules. Figure 7D shows the changes in the absorption and emission properties of Nile red encapsulated in vesicles of **1** in solution in aqueous medium in the presence of DNA. After addition of DNA, the spectrum of

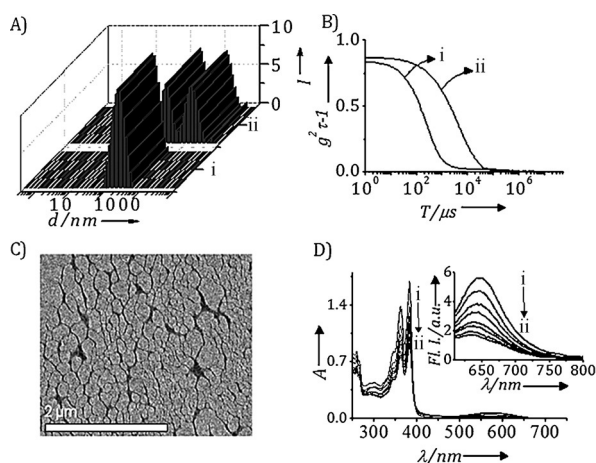


Figure 7. A) Size-distribution and B) correlation data of the conjugate 1 i) alone (0.4 mM) and ii) in the presence of ct-DNA (0.4 mM). C) TEM image of vesicles of conjugate 1 in the aqueous medium under similar conditions. D) Changes in the absorption and emission (inset) spectra of Nile red encapsulated in vesicles of conjugate 1 in aqueous medium upon addition of ct-DNA [$c = i) 0$ and $ii) 0.3$ mM].

the vesicles that contained Nile red showed considerable hypochromicity at $\lambda = 530$ nm, which corresponded to the released dye, with concomitant quenching of the fluorescence intensity at $\lambda = 630$ nm. These results demonstrate the potential of vesicles of conjugate 1 as carriers of hydrophobic dye molecules through an encapsulation–release process that uses DNA-stimulated disassembly.

Conclusion

Amphiphilic naphthalene imide conjugates 1 and 2 showed good solubility in the aqueous medium and exhibited significant DNA association constants ($K_{\text{DNA}} = 5\text{--}8 \times 10^4 \text{ M}^{-1}$) with intercalative binding interactions. Of these systems, NDI conjugate 1 exhibited vesicles in the aqueous medium at and above a CAC of 0.4 mM, whereas conjugate 2 aggregated to form lamellar flakes. The self-assembled vesicles of 1 encapsulated hydrophobic molecule Nile red efficiently. However, in the presence of DNA these vesicles disassembled, which was indicated by various photophysical and microscopic techniques. Uniquely, this transformation could be effectively employed to release the encapsulated hydrophobic molecules by using DNA as a stimulus. Thus, these conjugates exhibited their potential use as DNA probes, as well as potential carrier systems for the delivery of hydrophobic guest molecules in the aqueous medium.

Experimental Section

General techniques

The equipment and procedures for melting-point determination and spectral recordings are described elsewhere.^[19] All melting points are uncorrected and were determined with a Mel-Temp II melting-point apparatus. The electronic absorption spectra were

recorded with a Shimadzu UV-3101PC UV-Vis-NIR scanning spectrophotometer. Fluorescence spectra were recorded with a SPEX-Fluorolog F112X spectrofluorimeter. All experiments were carried out at room temperature (25 ± 1 °C), unless otherwise mentioned.

Materials and methods

Starting materials: NDA, NMA, 11-bromoundecanoic acid and ethanolamine were purchased from Aldrich and S. D. Fine Chemicals, India.

DNA-binding studies: The DNA-binding studies were performed in phosphate buffer (10 mM, pH 7.4) that contained NaCl (2, 50, 100 and 500 mM). K_{DNA} was determined by a half-reciprocal plot of $D/\Delta\varepsilon_{\text{ap}}$ versus D [Eq. (1)] by recording the absorbance at the respective maxima after each addition of ct-DNA.

$$D/\Delta\varepsilon_{\text{ap}} = D/\Delta\varepsilon + 1/(\Delta\varepsilon K_{\text{DNA}}) \quad (1)$$

D is the concentration of ct-DNA base pairs, $\Delta\varepsilon_{\text{ap}} = [\varepsilon_{\text{a}} - \varepsilon_{\text{f}}]$, $\Delta\varepsilon = [\varepsilon_{\text{b}} - \varepsilon_{\text{f}}]$,^[12] ε_{a} is the apparent extinction coefficient ($A_{\text{max}}/[\text{conjugate}]$), ε_{b} is the extinction coefficient of the bound form of the conjugate and ε_{f} is the extinction coefficient of the free conjugate. ε_{b} was determined from the gradient ($1/\Delta\varepsilon$) and K_{DNA} was obtained from the ratio of the slope to the y-intercept [$1/(\Delta\varepsilon K_{\text{DNA}})$].

Viscometric titrations were performed by using a LAUDA DLK10 automated viscometer, thermostat controlled at 25 °C in a constant-temperature bath. The concentration of ct-DNA was 0.3 mM, and the flow times were measured with an automated timer. Each sample was measured three times and an average flow time was calculated.

Determination of the CAC: The CAC values of 1 and 2 were determined by UV/Vis spectroscopy. A stock solution of 1 or 2 in water (5 mM) was prepared, and from this a series of solutions of various concentrations were made (46 μM –1.1 mM) and equilibrated for 2 h at RT before the analysis. The absorbance of 1 and 2 at $\lambda = 380$ and 340 nm, respectively, was plotted against concentration and the CAC value was estimated from the inflection point.

Encapsulation of Nile red by the vesicles of conjugate 1: A solution of Nile red in THF (3 mL, 0.1 mM) was placed in various glass vials and the solvent was evaporated. Solutions of various concentrations of 1 were added to the vials that contained Nile red, and the mixture was sonicated for 15 min and allowed to stand for 2 h before fluorescence spectroscopic analysis ($\lambda_{\text{ex}} = 530$ nm). The final concentration of Nile red was 100 μM and the emission intensity of encapsulated Nile red at $\lambda = 630$ nm was plotted versus the concentration of 1 and the inflection point of the plot was taken as the CAC of conjugate 1.

Acknowledgements

This work was supported by the Department of Science and Technology, New Delhi and the CSIR-National Institute for Interdisciplinary Science and Technology (CSIR-NIIST) (CSC 0134), Trivandrum. This is contribution PPG-363 from CSIR-NIIST, Trivandrum.

Keywords: amphiphiles • DNA binding • naphthalene imides • self-assembly • vesicles

- [1] a) J.-H. Fuhrhop, T. Wang, *Chem. Rev.* **2004**, *104*, 2901; b) X. Zhang, S. Rehm, M. M. Safont-Sempere, F. Würthner, *Nat. Chem.* **2009**, *1*, 623; c) L. Jiang, Z. Gao, L. Ye, A. Zhang, Z. Feng, *J. Biomater. Sci. Polym. Ed.* **2013**, *1*, 1282; d) M. R. Molla, S. Ghosh, *Phys. Chem. Chem. Phys.* **2014**, *16*, 26672.
- [2] a) D. F. Evans, H. Wennerstrom, *The Colloidal Domain: Where Physics, Chemistry, Biology, and Technology Meet*, 2nd ed., Wiley-VCH, Weinheim, **1999**; b) A. Sorrenti, O. Illa, R. M. Ortuño, *Chem. Soc. Rev.* **2013**, *42*, 8200.
- [3] a) J.-M. Lehn, *Science* **2002**, *295*, 2400; b) G. M. Whitesides, J. P. Mathias, C. T. Seto, *Science* **1991**, *254*, 1312; c) L. Brunsveld, B. J. B. Folmer, E. W. Meijer, R. P. Sijbesma, *Chem. Rev.* **2001**, *101*, 4071; d) Z. Chen, A. Lohr, C. R. Saha-Möller, F. Würthner, *Chem. Soc. Rev.* **2009**, *38*, 564.
- [4] a) C. Wang, Z. Wang, X. Zhang, *Acc. Chem. Res.* **2012**, *45*, 608; b) C. Wang, Z. Wang, X. Zhang, *Small* **2011**, *7*, 1379; c) P. Xing, T. Sun, A. Hao, *RSC Adv.* **2013**, *3*, 24776; d) Y. Kang, K. Liu, X. Zhang, *Langmuir* **2014**, *30*, 5989.
- [5] a) A. Almutairi, S. J. Guillaudeu, M. Y. Berezin, S. Achilefu, J. M. J. Fréchet, *J. Am. Chem. Soc.* **2008**, *130*, 444; b) Y. Bae, N. Nishiyama, K. Kataoka, *Bioconjugate Chem.* **2007**, *18*, 1131; c) C. Wang, K. C. Tam, R. D. Jenkins, C. B. Tan, *J. Phys. Chem. B* **2003**, *107*, 4667; d) S. Lecommandoux, O. Sandre, F. Checot, J. Rodriguez-Hernandez, R. Perzynski, *Adv. Mater.* **2005**, *17*, 712; e) D. Schmaljohann, *Adv. Drug Delivery Rev.* **2006**, *58*, 1655; f) A. P. de Silva, C. M. Dobbin, T. P. Vance, B. Wannalser, *Chem. Commun.* **2009**, 1386.
- [6] a) M. D. Burke, J. O. Park, M. Srinivasarao, S. A. Khan, *J. Controlled Release* **2005**, *104*, 141; b) P. D. Thornton, G. McConnell, R. V. Ulijn, *Chem. Commun.* **2005**, 5913; c) M. A. Azagarsamy, V. Yesilyurt, S. Thayumavan, *J. Am. Chem. Soc.* **2010**, *132*, 4550.
- [7] a) I. Saito, M. Takayama, S. Kawanishi, *J. Am. Chem. Soc.* **1995**, *117*, 5590; b) I. Saito, M. Takayama, H. Sugiyama, K. Nakatani, A. Tsuchida, M. Yamamoto, *J. Am. Chem. Soc.* **1995**, *117*, 6406; c) J. E. Rogers, S. J. Weiss, L. A. Kelly, *J. Am. Chem. Soc.* **2000**, *122*, 427; d) S. Banerjee, S. A. Bright, J. A. Smith, J. Burgeat, M. Martínez-Calvo, D. C. Williams, J. M. Kelly, T. Gunnlaugsson, *J. Org. Chem.* **2014**, *79*, 9272; e) S. Banerjee, E. B. Veale, C. M. Phelan, S. A. Murphy, G. M. Tocci, L. J. Gillespie, D. O. Frimannsson, J. M. Kelly, T. Gunnlaugsson, *Chem. Soc. Rev.* **2013**, *42*, 1601.
- [8] a) S. V. Bhosale, C. H. Janiab, S. J. Langford, *Chem. Soc. Rev.* **2008**, *37*, 331; b) A. Sikder, A. Das, S. Ghosh, *Angew. Chem. Int. Ed.* **2015**, *54*, 6755; *Angew. Chem.* **2015**, *127*, 6859.
- [9] a) M. R. Molla, D. Gehrig, L. Roy, V. Kamm, A. Paul, F. Laquai, S. Ghosh, *Chem. Eur. J.* **2014**, *20*, 760; b) C. Kulkarni, S. J. George, *Chem. Eur. J.* **2014**, *20*, 4537; c) P. Rajdev, M. R. Molla, S. Ghosh, *Langmuir* **2014**, *30*, 1969.
- [10] a) S. Banerjee, J. A. Kitchen, S. A. Bright, J. E. O'Brien, D. C. Williams, J. M. Kelly, T. Gunnlaugsson, *Chem. Commun.* **2013**, *49*, 8522; b) S. Roy, S. Saha, R. Majumdar, R. R. Dighe, A. R. Chakravarty, *Inorg. Chem.* **2009**, *48*, 9501; c) K. J. Kilpin, C. M. Clavel, F. Efade, P. J. Dyson, *Organometallics* **2012**, *31*, 7031.
- [11] a) M. R. Molla, S. Ghosh, *Chem. Eur. J.* **2012**, *18*, 9860; b) S. Mukherjee, H. Raghuraman, A. Chattopadhyay, *Biochim. Biophys. Acta Biomembr.* **2007**, *1768*, 59.
- [12] a) E. Kuruville, D. Ramaiah, *J. Phys. Chem. B* **2007**, *111*, 6549; b) J. Joseph, E. Kuruville, A. T. Achuthan, D. Ramaiah, G. B. Schuster, *Bioconjugate Chem.* **2004**, *15*, 1230; c) E. Kuruville, P. C. Nandajan, G. B. Schuster, D. Ramaiah, *Org. Lett.* **2008**, *10*, 4295; d) M. Hariharan, J. Joseph, D. Ramaiah, *J. Phys. Chem. B* **2006**, *110*, 24678; e) S. C. Karunakaran, D. Ramaiah, I. Schulz, B. Epe, *Photochem. Photobiol.* **2013**, *89*, 1100.
- [13] a) C. V. Kumar, E. H. Asuncion, *J. Am. Chem. Soc.* **1993**, *115*, 8547; b) P. P. Neelakandan, K. S. Sanju, D. Ramaiah, *Photochem. Photobiol.* **2010**, *86*, 282.
- [14] a) D. L. Boger, B. E. Fink, S. R. Brunette, W. C. Tse, M. P. Hedrick, *J. Am. Chem. Soc.* **2001**, *123*, 5878; b) N. C. Garbett, N. B. Hammond, D. E. Graves, *Biophys. J.* **2004**, *87*, 3974.
- [15] a) M. Nakamura, T. Okaue, T. Takada, K. Yamana, *Chem. Eur. J.* **2011**, *17*, 5344; b) N. C. Garbett, P. A. Ragazzon, J. B. Chaires, *Nat. Protoc.* **2007**, *2*, 3166.
- [16] a) A. Rodger, S. Taylor, G. Adlam, I. S. Blagbrough, I. S. Haworth, *Bioorg. Med. Chem.* **1995**, *3*, 861; b) A. Rodger, I. S. Blagbrough, G. Adlam, M. L. Carpenter, *Biopolymers* **1994**, *34*, 1583.
- [17] a) J.-Z. Wu, L. Yuanand, J.-F. Wu, *J. Inorg. Biochem.* **2005**, *99*, 2211; b) J. Talib, D. G. Harman, C. T. Dillon, J. A. Wright, J. L. Becka, S. F. Ralph, *Dalton Trans.* **2009**, 504; c) H. Ihmels, J. Mattay, F. May, L. Thomasa, *Org. Biomol. Chem.* **2013**, *11*, 5184.
- [18] a) F. P. Gasparro, *Psoralen DNA Photobiology*, CRC Press, Boca Raton, Florida, **1988**; b) D. J. Patel, L. Cannel, *Proc. Natl. Acad. Sci. USA* **1976**, *73*, 674.
- [19] a) R. R. Avirah, K. Jyothish, D. Ramaiah, *Org. Lett.* **2007**, *9*, 121; b) K. T. Arun, D. Ramaiah, *J. Phys. Chem. A* **2005**, *109*, 5571; c) D. D. Gayathri Devi, T. R. Cibir, D. Ramaiah, A. Abraham, *J. Photochem. Photobiol. B* **2008**, *92*, 153; d) K. T. Arun, D. T. Jayaram, R. R. Avirah, D. Ramaiah, *J. Phys. Chem. B* **2011**, *115*, 7122.

Received: July 28, 2015

Published online on October 22, 2015